TM-2256

Thoughts on Ion Trapping Instability in the Recycler

David Neuffer and K. Y. Ng
Fermilab

Abstract

Instabilities driven by ions (or electrons) trapped within the space charge potential of a circulating beam are common in accelerators and storage rings. In the recycler, the stored antiproton ($\bar{p}$) beam could trap positive ions (H_2^+, CO^+, etc.). Conditions for trapping are discussed, and trapping potentials are calculated. Ion trapping can be reduced by clearing electrodes, a beam-free gap (or gaps), and beam shaking. Tune shifts, coherent instabilities and other effects of trapped ions on stored $\bar{p}$'s are discussed. A "fast-ion" instability mode is also possible. Experiments to determine conditions and consequences of such instability in the recycler are discussed.

Introduction

Many accelerators and storage rings have observed trapped ions and electrons, and these can cause instabilities.[1,2,3] Beam particles hitting a vacuum gas molecule often cause ionization, typically producing a positive ion and an electron. Positive beam particles (protons, positrons) can trap electrons while negative beam particles (electrons, antiprotons) trap ions. Interactions with the trapped particles can cause instability and beam loss as well as emittance growth.

Both the CERN Antiproton Accumulator and the Fermilab Accumulator have measured trapped ions and their effects, and have used clearing mechanisms to control the problem. [4, 5] The Recycler Ring (RR) (or $\bar{P}$-Amplifier) has also had evidence for trapped ions, with accompanying emittance growth. In this note we discuss conditions for trapped ions in the RR, their potential effects, and possible clearing mechanisms. Comparisons with observations and future experiments are discussed.

Recycler ring [6] parameters are summarized in Table 1. The RR is composed of permanent magnets, so that the central momentum $P_{\bar{p}} = 8.89$ GeV/c is fixed. (Kinetic energy $T_{\bar{p}} = 8.0$ GeV.) The RR has a relatively large circumference ($L_{RR} \cong 3320$ m) and the beam compaction factor is $\eta_T = 1/\gamma^2 - 1/\gamma_T^2 = 1/9.53^2 - 1/20.0^2 = 0.0085$. In beam storage/cooling mode the beam is confined in a single long bunch by barrier bucket rf waveforms, with a typical bunch length of L_B = 2400m (8μs). As a reference energy spread we use $\sigma_E = 2.5$MeV ("90%" full width of 10.0 MeV), which, with the 8 μs bunch length, obtains a "90%" longitudinal emittance of ~80 eV-s. The very long bunch, with relatively weak rf, provide unique characteristics to beam in the RR, with potentially different instability modes. The RR lattice functions (β_x, β_y, η) are shown in figure 1 and β_x, β_y oscillate between ~15 and 55m, while the dispersion η oscillates between 0.0 and 0.5m. We use an rms normalized emittance of $\varepsilon_{N,rms} = 1.6$ πmm-mrad to set the reference beam sizes. (95% emittance is 10 πmm-mrad.) The rms beam sizes, obtained from:

$$\sigma = \sqrt{\varepsilon_{N,rms}\beta_\perp / \gamma_{\bar{p}}\beta_{\bar{p}}} \quad ,$$

vary from ~1.6 to 3.0 mm. In operation, rms emittances from 3 to 6 πmm-mrad have been recently obtained in the RR, and that would reduce beam sizes to as small as 0.9 to 1.6 mm.

Ion production and loss mechanisms

After improvements, the recycler vacuum pressure is typically ~1—10×10^{-10} Torr, and consists of H_2, CO, N_2, H_2O, Ar, … For the present calculations we will use 10^{-10} Torr as a reference value, and calculate effects from that value. The gas particle density n_X is given by:

$$n_X = \frac{P}{R_S T}$$

where $R_S = 1.0356\times10^{-25}$ m^3-K/Torr, P is the pressure in Torr, T the temperature in Kelvin. For P = 10^{-10} Torr and T = 300° K, we obtain $n_X \cong 3.2\times10^{12}$ ions/m^3. We will also use H_2^+ as a reference light ion and CO^+ as a reference heavy ion; effects of ions of similar mass will be very similar. Trapped ion effects have been observed when $N_{\bar{p}} = 20\times10^{10}$ $\bar{p}$'s are stored in the RR, and we use that as an intial reference value. In operation, the RR will store 200—600×10^{10} $\bar{p}$'s , and some instability effects will become much worse at these intensities, as discussed below. The ionization cross section for $\bar{p}$ – CO ionization is $\sigma_{CO} \cong 10^{-22}$ m^2, while the cross section for $\bar{p}$ –H_2 ionization is $\sigma_{H2} \cong 0.2\times10^{-22}$ m^2. [7] The rate of ion production is given by $R_x = N_{\bar{p}}\, \sigma_x\, n_x\, L_{acc}$ ions per turn. At 10^{-10} Torr and $N_{\bar{p}} = 20\times10^{10}$, this is ~$2.1\times10^5$ CO^+ and 4.2×10^4 H_2^+ per turn. (1 turn = 11.13 μs.), and the beam could become fully neutralized after 10–50 s.

A number of effects can reduce ion accumulation. Collisions with molecules and ions can neutralize or further ionize them. Beam-ion collisions can also further ionize the beam. The cross-sections for these effects are similar to the initial ionization cross-section. Ions can only accumulate until the trapped charge density is equal to the beam density. Without clearing, however, the CERN AA and Fermilab Accumulator accumulate an ion density that approaches the beam density, and we would expect similar behavior in the RR. In the next section we discuss the trapping and clearing mechanisms.

Ion potential and clearing electrodes

Ions are produced with an initial kinetic energy similar to the thermal energy (1.5kT), which is ~0.04 eV at 300°K. The negatively-charged $\bar{p}$ beam forms a potential well which can trap ions The long bunch structure in the RR spreads the beam over a long distance, developing a very weak potential well. The well is still greater than the ion thermal energy and will still trap ions.

The potential well depth can be calculated using Maxwell's equations, for various particle distributions and beam-pipe geometries. The simplest case is to assume a round beam of constant density within the radius r_{beam} within a round beam pipe of radius r_c. The linear density is $\lambda = e\, N_{\bar{p}}/L_{bunch}$. The potential U(r) is:

$$U = \frac{\lambda}{2\pi\varepsilon_0}\ln\left(\frac{r}{r_c}\right) \qquad r > r_{beam}$$

$$U = \frac{\lambda}{2\pi\varepsilon_0}\left[\frac{r^2}{2\,r_{beam}^2} - \frac{1}{2} + \ln\left(\frac{r_{beam}}{r_c}\right)\right] \qquad r < r_{beam}$$

With $N_{\bar{p}} = 20\times10^{10}$, L_{bunch} = 2400m, r_{beam} = 4.5mm and r_c = (2.25+4.5)/2 cm, we find U(0) = –0.62 V.
A slightly different potential is obtained with a Gaussian round beam. The potential can be calculated using:

$$U(r) = -\int_r^{r_c} \frac{\lambda}{2\pi\varepsilon_0} \frac{1-e^{-\frac{r^2}{\sigma_r^2}}}{r} dr$$

obtaining:

$$U(r) = -\frac{\lambda}{2\pi\varepsilon_0}\left(\left[\frac{\Gamma(0,\frac{r^2}{\sigma_r^2}) - \Gamma(0,\frac{r_c^2}{\sigma_r^2})}{2}\right] + \ln\left[\frac{r_c}{r}\right]\right)$$

This provides a slightly different potential profile U(r) from the constant-density case. Figure 2 compares the two examples (at $\sigma_r = r_{beam}/\sqrt{2}$, and $r_c = 10\sigma_r$). At RR parameters the change in minimum potentials is < 5%.

The RR beam pipe is elliptical with a full width (2b) of ~9cm and a full height (2a) of ~4.5cm. We were unable to find a simple solution for that more complicated geometry (elliptical Gaussian beam within elliptical beam pipe). Grobner and Hubner approximated this for the ISR with a rectangular beam within a rectangular beam pipe.[8] The expression for the potential V at the center of the pipe is:

$$V(0) = \sum_{s=1}^{\infty}\left(1 - \frac{\cosh\left[\frac{\pi s}{2w}(h-b))\right]}{\cosh\left[\frac{\pi s}{2w}h\right]}\right) C_s \sin\left(\frac{\pi}{2}s\right)$$

,

where the coefficient C_s is given by the expression:

$$C_s = \frac{2\lambda w^2}{\varepsilon_o a\, b\, \pi^3 s^3} \frac{\cos\left(\frac{\pi s}{2w}(w-a)\right) - \cos\left(\frac{\pi s}{2w}(w+a)\right)}{\left(1 - \frac{s^2 a^2}{4w^2}\right)}$$

In these expressions, s is a summation integer, a is the beam half-width, b is the beam half-height, 2w is the pipe width and 2h is the pipe height.

This expression has been evaluated around the RR, using the reference values ($N_{\bar{p}} = 20\times10^{10}$, L_{bunch} = 2400m, $\varepsilon_{N,rms}$ = 1.6 mm-mrad, and a 4.5×9cm beam pipe). The results are displayed in figure 3. The variation is relatively small, because the beam size is relatively constant and the beam pipe has a constant cross-section. The maximum trapping voltages occur near the vertical beam size minima, with more enhancement where horizontal beam sizes are also relatively small. Other accelerators (ISR, $\bar{p}$ accumulator) have larger variations due to beam pipe changes and larger beam size variations.

To remove ions, clearing electrodes are installed in the RR beam position monitors (BPMs). In the arcs, these are located in the straight sections adjacent to the combined function magnets that provide bending and focusing for the $\bar{p}$'s. The combined-function magnets are placed in pairs

with no clearing within or between the magnets. The magnet pair is ~11.5m long and the straight section is ~5m long. Ions created within the magnet pair would have their motion significantly controlled by the magnetic fields, confining them in Larmor orbits around the field lines, and ions created within the intermagnet gap would be trapped between the magnets. Clearing would be relatively ineffective in the magnet region. Ion neutralization should be relatively high within and between magnets, and the magnets cover more than half the RR circumference.

Ions must drift to the clearing electrode to be removed and the electrode spacing L is ~10m in the RR. The time required for ions to be cleared is $t_{clear} \sim L/(v_{rms})$ or ~0.02s, if L=10m and $v_{vrms}= (3\ k\ T/\ M_{ion})^{1/2} \cong 500$ m/s (for CO^+). The net neutralizaton, assuming freely drifting ions, would be the drift clearing time divided by the ion production time, or ~0.002 to 0.02 for CO^+ ions at 10^{-10} to 10^{-9} Torr, respectively.

Ion trapping/detrapping

For ions to remain trapped, they must remain within the space charge potential well of the beam. For small oscillations about the center of the potential well, the transverse motion of the ions within that potential well is:

$$\frac{d^2y}{dt^2} = -\frac{e^2 N_{\bar{p}}(1-\eta)}{2\pi\varepsilon_0 L_1 A m_p \sigma_y(\sigma_x+\sigma_y)} y$$

Here $N_{\bar{p}}/L_1$ is the $\bar{p}$ beam intensity, σ_x, σ_y the rms beam sizes and η is the neutralization.

The barrier-bucket rf in the RR forms the $\bar{p}$'s into a long bunch of length L_1 ~ constant intensity, followed a beam-free gap of length L_2, with $L_1 + L_2$ equal to the RR circumference L_{acc}. The ions are at a fixed position within the ring and see a long bunch, which focuses the beam, followed by a beam-free gap, without focusing (as shown in fig. 5). The sequence of focusing and nonfocusing can be represented as a transport matrix, written as (with $\eta = 0$):

$$M = \begin{bmatrix} 1 & L_2 \\ 0 & 1 \end{bmatrix} \begin{bmatrix} \cos(kL_1) & \frac{1}{k}\sin(kL_1) \\ -k\sin(kL_1) & \cos(kL_1) \end{bmatrix}$$

where:

$$k = \sqrt{\frac{2r_p N_{\bar{p}}(1-\eta)}{\beta^2 A L_1 \sigma_y(\sigma_x+\sigma_y)}}$$

Trapping requires stability of motion in this matrix representation, which requires:

$$|\mathrm{Tr}\ M|/2 \le 1 \quad .$$

At RR parameters this is often not true. The motion tends to become unstable when the ions are strongly overfocused within the beam and when the unfocusing gap (L_2) is relatively large. Thus low-A ions at larger $\bar{p}$-intensities would tend to be detrapped by the gap. The reference values (A=28, L_1=2400m, $N_{\bar{p}}=20\times10^{10}$) tend to be near the threshold for trapping/detrapping, so we expect conditions for ion trapping to exist in much of the ring circumference, with relatively small changes in parameters increasing or decreasing the amount of trapping. At the reference values, the stability criterion is met in vertical motion for ~50% of the ring circumference, and simultaneously for vertical and horizontal for ~10%.

With $\eta > 0$, this expression should be written to reflect the alternation of focusing from $\bar{p}$'s and defocusing from other ions, obtaining:

$$M = \begin{bmatrix} \cosh(k_2 L_2) & \frac{1}{k_2}\sinh(k_2 L_2) \\ k_2 \sinh(k_2 L_2) & \cosh(k_2 L_2) \end{bmatrix} \begin{bmatrix} \cos(kL_1) & \frac{1}{k}\sin(kL_1) \\ -k\sin(kL_1) & \cos(kL_1) \end{bmatrix} \tag{1}$$

with:

$$k_2 = \sqrt{\frac{2 r_p N_{\bar{p}} \eta}{\beta^2 A L_1 \sigma_y (\sigma_x + \sigma_y)}}$$

At RR parameters, the beam often becomes more stably trapped as the neutralization factor η increases (for η <~0.75), since the stability conditions are near threshold, and the ions reduce the overfocusing.

The behavior is also critically dependent on $N_{\bar{p}}$. At $N_{\bar{p}} = 200\times10^{10}$, the ions can be much more strongly overfocused, and ions are more easily cleared by the gap.

Effects of beam in gap

In the previous discussion we assumed the $\bar{p}$–beam was confined to the bunch length L_1, with no $\bar{p}$'s in the interbunch gap. It has been noted experimentally that reducing the rf voltage to a small value, and thereby letting beam into the interbunch gap, makes the beam more unstable. This could be due to the fact that the partially filled gap maintains ion trapping.

The ion trapping conditions can be extended to include the effect of a partially filled gap by including a non zero density of beam in the gap, which we can write as $\lambda_{gap} = \alpha\, \lambda_{bunch} = \alpha\, N_{\bar{p}}/L_1$. Note that, with this notation convention, the total number of $\bar{p}$'s in the bunch + gap is:

$$N_{total} = N_{bunch} + N_{gap} = N_{\bar{p}}\left(1 + \alpha \frac{L_2}{L_1}\right)$$

In this notation, the focusing factor k_2 is written as:

$$k_2 = \sqrt{\frac{2 r_p N_{\bar{p}} |\eta - \alpha|}{\beta^2 A L_1 \sigma_y (\sigma_x + \sigma_y)}}$$

For $\eta > \alpha$, the gap is defocusing and the same matrix used above in eq. (1) is used. If $\alpha > \eta$, then the gap is focusing and the "single-turn" transport is the product of two focusing matrices:

$$M = \begin{bmatrix} \cos(k_2 L_2) & \frac{1}{k_2}\sin(k_2 L_2) \\ -k_2 \sin(k_2 L_2) & \cos(k_2 L_2) \end{bmatrix} \begin{bmatrix} \cos(kL_1) & \frac{1}{k}\sin(kL_1) \\ -k\sin(kL_1) & \cos(kL_1) \end{bmatrix}$$

This double-focusing matrix is more likely to have stable trapping than the previous (gap-neutral and gap-defocusing) cases, particularly when the gap focusing is relatively large (η > ~0.1).

Ion effects

The accumulated ions affect the motion of the $\bar{p}$'s in the RR. The ions would focus the $\bar{p}$'s, canceling (or over-canceling) the space charge defocusing. The lowest order effect is a space charge tune shift, which is amplitude-dependent.[9] The zero-amplitude tune shift is:

$$\Delta\nu_{y,\mathrm{direct}(\mathrm{ion}+\bar{p})} = \frac{F_z\, r_p N_{\bar{p}}}{2\pi\beta^2\gamma}\left\langle \frac{\beta_y}{\sigma_y(\sigma_y+\sigma_x)}\right\rangle\left(\frac{1}{\gamma^2}-\eta\right)$$

where F_z is a factor of order unity that depends on the beam distribution, η is the neutralization factor (ratio of ion to beam density), β_y is the betatron function, and the carats indicate averaging around the ring. For round beams this becomes:

$$\Delta\nu_{y,\mathrm{direct}(\mathrm{ion}+\bar{p})} \cong \frac{r_p N_{\bar{p}}}{2\pi}\frac{1}{2\varepsilon_{N,\mathrm{rms}}}\left(\frac{1}{\gamma^2}-\eta\right)$$

The direct $\bar{p}$ space charge force is in the $1/\gamma^2$ term, while the ion defocusing is the $-\eta$ term. The $1/\gamma^2$ derives from the sum of the magnetic and electric fields from the $\bar{p}$ beam charge and current. The ions, which are motionless in the lab contribute only an electric field. In the RR, $\gamma \cong 9.53$. If η is greater than ~0.01, the neutralization tune shift is greater than the direct space charge tune shift. At $N_{\bar{p}} = 20\times10^{10}$, $\varepsilon_{N,\mathrm{rms}} = 1.6\times10^{-6}$ πm-rad this expression becomes:

$$\Delta\nu_{y,\mathrm{direct}(\mathrm{ion}+\bar{p})} \cong 0.015\left(\frac{1}{\gamma^2}-\eta\right)$$

This tune shift can be greatly increased if $\varepsilon_{N,\mathrm{rms}}$ is cooled and $N_{\bar{p}}$ is increased. The RR has operated at $N_{\bar{p}} = 120\times10^{10}$ and $\varepsilon_N = 0.5\times10^{-6}$, which would increase this factor to:

$$\Delta\nu_{y,\mathrm{direct}(\mathrm{ion}+\bar{p})} \cong 0.30\left(\frac{1}{\gamma^2}-\eta\right),$$

which is ~-0.08 at $\eta = 0.3$, and could shift the tune fairly close to the half-integer resonance, as noted by Balbekov.[10]

When the RR ring intensity is increased to 200 or 600 $\times10^{10}$ the space charge is proportionately larger, and relatively small neutralizations can lead to large tune shifts. ($\Delta\nu = 0.07$ at η=0.1, $N_{\bar{p}} = 600\times10^{10}$, $\varepsilon_{N,\mathrm{rms}} = 1.0\times10^{-6}$ πm-rad.)

Tune shifts have been measured in the CERN AA and Fermilab accumulator, as a signal that ion trapping is occurring and to measure the effectiveness of clearing in reducing ion trapping. Similar measurements should be obtained in the RR.[11]

The large tune shifts can lead to increase of emittance (which would reduce $\Delta\nu \propto N_{\bar{p}}/\varepsilon_{N,\mathrm{rms}}$ to a dynamically tolerable level) and beam instability, particularly if the tune is near resonances.

Ion-beam oscillations

Ions trapped within the beam perform stable oscillations. In the small-amplitude, linearized limit the equation of motion is:

$$\frac{d^2y}{dt^2} = -\frac{e^2 N_{\bar{p}}(1-\eta)}{2\pi\varepsilon_0 L_1 A m_p \sigma_y(\sigma_x+\sigma_y)} y = -q_I^2\omega_0^2 y \quad ,$$

where q_I is the "tune" of the ion oscillations, and $\omega_0 = c/R$ is the angular $\bar{p}$ revolution frequency. q_I can be written as:

$$q_I = \sqrt{\frac{2R^2 r_p N_{\bar{p}}(1-\eta)}{L_1 A\sigma_y(\sigma_x+\sigma_y)}} \quad .$$

At reference values ($\sigma_x = \sigma_y = 2.24$mm, L_1=2400m, $N_{\bar{p}}=20\times10^{10}$), the ion oscillation frequency is 170 kHz ($q_I = 1.89$) for H_2^+ ions and 45.6kHz (q_I=0.51) for CO^+. These frequencies vary around the ring, depending on σ_x, σ_y and are also amplitude dependent, with the zero-amplitude frequency usually the highest. Fig. 3 shows these frequencies around the ring.

The $\bar{p}$'s circulating in the ring have focusing betatron oscillations as well as coupled oscillations with the trapped ions. These coupled oscillations can cause instabilities.

Keil and Zotter have developed a model for linearized coupled oscillations and derived conditions for instability.[12, 13] We follow that model in the following discussion. The equation of motion for ions trapped within the $\bar{p}$ beam is:

$$\frac{d^2X_I}{dt^2} + q_I^2\omega_0^2 X_I = q_I^2\omega_0^2\overline{X_{\bar{p}}}$$

where X_I is the ion transverse coordinate (x or y), $X_{\bar{p}}$ is the $\bar{p}$ transverse coordinate, and $\overline{X}_I, \overline{X}_{\bar{p}}$ indicate the centroids of the ion and $\bar{p}$ beams. The equation for $\bar{p}$ motion is:

$$\frac{d^2X_{\bar{p}}}{dt^2} + (Q^2+Q_{\bar{p}}^2)\omega_0^2 X_{\bar{p}} = Q_{\bar{p}}^2\omega_0^2\overline{X_I}$$

where Q is the betatron tune and $Q_{\bar{p}}$ indicates the $\bar{p}$ oscillation within the ion beam field:

$$Q_{\bar{p}}^2\omega_0^2 = \frac{N_I r_p c^2}{\pi\gamma r_{beam}^2 R}$$

where $N_I = \eta N_{\bar{p}}$. Note that in this formula we have made the approximations of round beams and constant ion and beam density (no gap), as well as relativistic $\bar{p}$ motion. We have also used the expressions for oscillation within a uniform density with radius r_{beam} for both ions and $\bar{p}$'s. Under these approximations, $q_I^2 = Q_{\bar{p}}^2\,\gamma(1-\eta)/(\eta A)$.

The transverse motion for the ions is fixed in space and oscillates in time; the $\bar{p}$ motion changes around the ring as well as oscillating in time. We are interested in resonant harmonics of coupled motion:

$$X_I = a_I e^{-i\omega t} \quad , \; X_{\bar{p}} = a_{\bar{p}} e^{i(n\theta - \omega t)}$$

where a_I, $a_{\bar{p}}$ indicate particle amplitudes, and $\theta = \omega_0 t$. With this ansatz, we can solve the coupled equations of motion for ω, obtaining a quartic equation:

$$\left(W^2 - q_I^2\right)\left((W-n)^2 - (Q^2 + Q_{\bar{p}}^2)\right) = Q_{\bar{p}}^2 q_I^2$$

where $W = \omega/\omega_0$. Since $Q_{\bar{p}} << Q$, we can ignore it (or slightly shift the value of Q) in the sum $Q^2+Q_{\bar{p}}^2$. Unstable values (complex W) can occur where $W \cong n\text{-}Q$, and where $q_I \cong n\text{-}Q$. With these conditions and $W=n\text{-}Q+\delta$ the above equation becomes quadratic in δ:

$$\delta^2 + \left((n-Q) - q_I\right)\delta + \frac{Q_{\bar{p}}^2 q_I}{4Q} \cong 0$$

which has complex solutions if:

$$\delta Q = \left|(n-Q) - q_I\right| < \sqrt{\frac{Q_{\bar{p}}^2 q_I}{Q}} \cong \sqrt{\frac{\eta A q_I^3}{\gamma Q}} \; .$$

At the reference RR operating values, $q_I \cong 0.5$, and it varies around the ring with values between ~0.4 and ~0.6. (see fig. 3) Instability can occur if some portion of the ring has δQ less than the expression on the right and greater than the Landau damping tune spread. A typical tune spread could be ~0.02. The tune Q is 24.415, so the smallest value of n-Q is 0.585, which is within the ion oscillation frequency spread. If we use $\delta Q = 0.02$, it is relatively easy for the instability criterion to be met; $\eta^{1/2} > \sim 0.125$ ($\eta > \sim 0.02$). Relatively weak neutralization can generate instability. Instability at weak neutralization does require that $n\text{-}Q\text{-}q_I$ be quite small, which means that q_I must be close to 0.585, or 1.585 or 2.585. This may imply that there will be bands of intensity (corresponding to the different resonances) where instability with small neutralization could occur.

The oscillations can be damped if the product of the $\bar{p}$ beam tune spread $\Delta_{\bar{p}}$ and the ion oscillation tune spread Δ_I is greater than the square of δQ:

$$\Delta_{\bar{p}} \Delta_I > \left| \frac{q_I^3 \eta A}{Q\gamma} \right|$$

If the $\bar{p}$ tune spread be dominated by chromaticity:

$$\Delta_{\bar{p}} \cong \left| Q\xi \frac{\delta p}{p} \right|$$

and with $\Delta_I \cong q_I$, then, at $\delta Q = 0.02$ and $q_I \cong 0.6$, $Q\xi\, \delta p/p > \sim 0.001$ is required. At $\delta p/p = 3\times10^{-4}$, $Q\xi > \sim 3$ is required. This is similar to the chromaticities needed to stabilize the observed instability.

The analysis of the present section shows that, if significant neutralization occurs ($\eta > \sim 0.02$), resonant unstable amplitude growth can occur. The instability can be somewhat controlled by chromaticity.

"Fast-Ion" Instability

Raubenheimer and Zimmermann have noted an ion-beam instability mode that occurs even if ions are not trapped for multiple turns within a circulating beam.[14, 15] This "fast-ion" instability has been observed in long trains of bunches in high-intensity electron storage rings. [16, 17]

In the "fast-ion" instability, the long bunch ionizes the background gas, with the ion density increasing as the head to the tail of the bunch pass through the gas and more ions are produced and trapped. (see figure 7) Coupled oscillations between ions and beam appear which increase toward the end of the bunch. After the bunch end passes, the ions are no longer trapped, and clear from the beam pipe. This pattern of ion buildup occurs throughout the multiturn transport, and instability effects such as emittance growth can occur. The instability process could occur in the RR, where the use of a very long bunch enables significant single-pass oscillation growth, which can then accumulate statistically over many turns, causing emittance growth.

In the present discussion we follow the presentation of A. Chao.[18] The instability is expected to be greatest when the $\bar{p}$ beam is at highest intensity and the vacuum is relatively weak. We will therefore use reference values of $N_{\bar{p}} = 200\times10^{10}$ and $P_{vac} = 10^{-9}$ Torr. The ion density λ_{ion} produced by a single passage of the beam bunch is:

$$\lambda_{ion} = \sigma_{CO} n_{CO} N_{\bar{p}} \cong 6.4\times10^{3} \quad \text{ions/m}$$

Here we have used CO as the representative background gas component. (One can sum over existing gas species.) This ion density increases linearly as the bunch passes through the gas.

As in the above treatment with a relatively constant ion density, one obtains coupled oscillations between the circulating $\bar{p}$ bunch and the transitory ions. The ions oscillate within the focusing force of the $\bar{p}$-beam:

$$\frac{\partial^2}{\partial t^2} y_I(s,t,z_1) + \omega_I^2 \left[y_I(s,t,z_1) - y_{\bar{p}}(s, ct-s) \right] = 0$$

Here y_I is the ion centroid coordinate and $y_{\bar{p}}$ is the beam centroid, $\omega_I^2 = (2N_{\bar{p}} r_p c^2)/(AL_{bunch} a^2)$ determines the oscillation frequency of ions in the $\bar{p}$-bunch with length L_{bunch}, and transverse radius a. The ions are located at longitudinal position s and evaluated at time t, where $\bar{p}$'s at position $z = ct - s$ along the bunch are passing by. The parameter z_1 indicates the ion creation time, where their rms position matches that of the $\bar{p}$-beam passing through them.

The equation of motion for the $\bar{p}$'s, which includes betatron oscillation and coupled ion-$\bar{p}$ oscillation is:

$$c^2 \frac{\partial^2}{\partial s^2} y_{\bar{p}}(s,z) + \omega_\beta^2 y_{\bar{p}}(s,z) + \frac{Kz}{L_{bunch}} \left[y_{\bar{p}}(s,z) - \int_0^z y_I(s,(s+z)/t,z_1)\,dz_1 \right]$$

where $K = 4\,\lambda_{ion} c^2 r_p/\gamma a^2$ gives the oscillation of $\bar{p}$'s within the ion density at the end of the bunch, and the z/L_{bunch} factor tracks the increase in ion density along the bunch length.

As in the previous analysis one assumes perturbed oscillatory motion for the $\bar{p}$'s,:

$$y_{\bar{p}}(s,z) \approx y_0(s,z) e^{-i\omega_\beta s/c + ikz}$$

with resonance motion at $kc \cong \omega_I$. After some algebra and approximations, we obtain a simplified equation for the amplitude y_0:

$$\frac{\partial^2}{\partial s \partial z} y_0(s,z) - \frac{K\omega_I}{4\omega_\beta c^2 L_{bunch}} z\, y_0(s,z) \approx 0$$

This equation has a relatively simple solution in terms of a single dimensionless variable:

$y_0(s,z) = y_0\ I_0(\eta_s)$, where $\eta_s = \frac{z}{c}\sqrt{\frac{K\omega_I s}{2\omega_\beta L_{bunch}}}$ and $I_0(z)$ is the Bessel function.

For large η_s (large s), this becomes:

$$y_0(s,z) \cong \frac{y_0 e^{\eta_s}}{\sqrt{2\pi\eta_s}}$$

The factor in the exponent can be rewritten as:

$$\eta_s = \frac{z}{L_{bunch}} \sqrt{\frac{s\ K\omega_I L_{bunch}}{2\omega_\beta c^2}}$$

In this expression, z is position along the bunch ($0 < z < L_{bunch}$), and s is distance of travel. (Time of travel is $\cong$ s/c.) The instability amplitude is largest toward the end of the bunch, and the rate of increase is not exponential in time, but follows $\exp[(t^{1/2})]$.

A characteristic growth distance s_C can be defined as the distance over which the amplitude has grown by a factor of e,:

$$s_C = \frac{2\omega_\beta c^2}{K\omega_I L_{bunch}} .$$

As reference values, we set a = 0.002m, L_{bunch} =1500m, $N_{\bar{p}} = 200\times10^{10}$, $P_{vac} = 10^{-9}$ Torr, $\Sigma_{ion} = 1.0\times10^{-22}$ m^2, A=28. For these parameters, $s_C \cong 9.98\times10^6$ m. The characteristic growth time t_C is $s_C/c = 3.3\times10^{-2}$ s. The expression for t_C can be rewritten as:

$$t_C = \left[\frac{\gamma_r}{(2r_p)^{3/2}\beta_{\perp,ave} c}\right]\left[\frac{A^{1/2}}{\Sigma_{ion}\, n_{gas}}\right]\left[\frac{a^3}{N_{\bar{p}}^{3/2} L_{bunch}^{1/2}}\right],$$

where the first bracketed term indicates the ring properties, the second term reflects the ion properties, and last term groups the $\bar{p}$-beam parameters.

Fast-Ion frequency spread, and damping

The instability is moderated by the frequency spread in the beam and also interacts with a damping system.

Stupakov[19] and Bosch [20] have considered the effect of ion frequency spread, and found that the frequency spread changes the character of the instability to be more clearly exponential:

$$y(s,z) \propto e^{\left(\frac{s}{c\tau_2}\frac{z}{L_{bunch}}\right)}$$

where

$$\tau_2 \cong t_C \frac{L_{bunch}\sigma_{\omega_i}}{c}\sqrt{\frac{8}{\pi}}\,.$$

In this expression $\sigma_{\omega i}$ indicates the ion frequency spread, which one expects to be some significant fraction of ω_I. For a broad frequency distribution ($\sigma_{\omega i}/\omega_I \cong (\pi/8)^{1/2}$), we find $\tau_2 \cong (2\omega_\beta)/K$, which is the inverse of the incoherent betatron frequency shift due to the ions (at $z = L_{beam}$) . At typical RR parameters this growth time is a few times larger than the single-frequency growth time (t_C).

Heifets has considered saturation effects, which are expected to occur if the oscillation amplitude becomes larger than the rms beam sizes σ_x, σ_y.[21] At large amplitudes the oscillations grow linear in time, with a characteristic time:

$$\tau_H \approx t_C \frac{\omega_I L_{bunch}}{c}$$

This would reduce the growth rate by ~ a factor of 10 from the small amplitude exponential growth rate.

In electron storage rings, the fast-ion instability is damped by radiation damping. Radiation damping for $\bar{p}$'s is too small, but we do have transverse stochastic cooling systems and could add a fast transverse damper. If the damping time were comparable to or smaller than the beam-ion growth time, the instability could be effectively controlled.

Stupakov and Chao have considered the effect of damping and the fast-ion instability.[22] The damper introduces a coherent damping term for the transverse oscillations, with damping time τ_D, as well as a heating term from noise in the damping system.

In a simplest model, the damping multiplies the oscillation by $\exp(-s/c\tau_D)$ where τ_D is the damping time. Since the growth is not fully exponential the damping time does not have to be smaller than the characteristic time t_C to be effective, although it should not be much larger.

In a more complicated model which includes amplifier noise heating as well as damping, the critical parameter is $\eta_{SC} = z/L_{bunch} \times (\tau_D/t_C)^{1/2}$. For $\eta_{SC} >> 1$, the amplitude growth follows an exponential:

$$\left\langle y^2(s,z)\right\rangle \cong F\frac{(c\tau_D)^{3/2}}{8L_{bunch}(ct_C)^{1/2}}\frac{e^{\eta_{SC}^2}}{\eta_{SC}},$$

where F is proportional to the initial noise amplitude.

For small η_{SC}, it follows a cubic relationship:

$$\left\langle y^2(s,z)\right\rangle \cong F\frac{z^3c^3\tau_D^3}{48L_{bunch}^4c^2t_c^2}$$

The two asymptotic dependences are shown in figure 8. The instability remains small if $\tau_D < t_C$, but grows exponentially toward the tail of the beam if $t_C < \tau_D$.

The "head-tail" model of the fast-ion instability can be disrupted by longitudinal beam motion. This means that, for fast-ion instability to occur, the growth time must be substantially less than the synchrotron period. The RR has a barrier-bucket bunching system, with an rf-free center (within $L_{gap} \cong L_{bunch}$) and a restoring voltage V_{BB} outside the gap. The synchrotron period is dependent upon the beam particle energy offset δ_E within the gap, and is given by:

$$T_{synch} = \frac{L_{acc}}{c}\left(\frac{2L_{gap}E}{L_{acc}\eta_{tr}\delta_E} + \frac{4\delta_E}{eV_{BB}}\right),$$

where $\eta_{tr} = 1/\gamma^2 - 1/\gamma_T^2 \cong 0.00886$, and we have used the relativistic approximation $\beta \cong 1$.

At typical RR parameters, $T_{synch} \cong 3$ to 10s, and this is somewhat larger that the "typical" fast beam ion instability time of ~0.03s. It is not decisively larger, so relatively smaller synchrotron periods (smaller L_{gap}, larger δ_E) coupled with larger instability times t_0 (smaller $P_{torr,}$, $N_{\bar{p}}$, larger σ_x, σ_y) could control the instability.

The Fast Beam Ion Instability is likely to occur in the RR and a future note will study this mode further to determine more accurately the conditions for the instability and to establish the bases for experimental observations and discuss possible remedies.

Observations/etc.

Instabilities have been observed in the RR under various conditions, and some observations are consistent with the hypothesis that the instabilities may be ion-$\bar{p}$ driven (multiturn and/or possibly "fast-ion"). [23]

One instability mode occurs at relatively low intensity. In this mode the beam intensity can be relatively small (~20—30 $\times 10^{10}$ $\bar{p}$'s), the bunch is long (>9 μs), and the rf is turned off to allow $\bar{p}$'s to leak into the interbunch gap. The transverse emittance increases with growth times of several minutes. Low frequency sidebands were seen in one experiment. Figure 9 shows the growth of x and y emittances in a RR experiment.

This instability seems most consistent with the multiturn ion-beam instability. It appears to require small momentum spread and small chromaticity, and it appears to be Landau-damped with larger momentum spread and chromaticity.

A separate (perhaps related) instability mode is seen at relatively high intensity (~120×10^{10} $\bar{p}$'s), appearing spontaneously on April 27 and triggered on May 5. The symptom is a fast transverse blow-up and beam loss event. The time scale for the event is less than a few seconds. It appears to require cooling of the beam to small transverse emittances and energy spread ($\varepsilon_{N,rms}$ < ~0.5 mm-mrad and δE_{rms} < 3 MeV). Unlike the previous slow instability mode it does not require debunched beam (rf off). It has been observed with the beam at a bunch length of 5.2μs. In an earlier example (March 8) the instability was seen with moderate intensity (~30×10^{10} $\bar{p}$'s), and long bunch (9.3μs) as well as small emittances and energy spread ($\varepsilon_{N,rms}$ < ~0.5 mm-mrad and δE_{rms} < 1.5 MeV) (see Fig. 10). In the cases where it has been observed, ~5% of the beam is lost and the rms emittance is doubled. Since the ring acceptance is much larger than that emittance, the perturbed distribution must be highly nonlinear with much of the beam unperturbed and some of it scattered to very large amplitudes.

This instability could be a "fast-ion" instability, although the speed and amplitude of the observed instability appear relatively large for the process. The alternative possibility of an impedance-driven instability is not excluded.

If it were a fast-ion instability, beam would be lost from the tail of the bunch. A fast-ion mode could explain the distribution observations, in that the head of the bunch would be unperturbed while the tail could be driven to large amplitudes.

The spectrum of the instability is not yet fully determined. Sidebands of the lower harmonics were seen, but they were not very large, and higher frequencies have not yet been explored. If the instability were driven by CO oscillations, the frequency of oscillations would be ~250 kHz in the April 27 instability, and would drop off at higher frequencies (> ~500kHz).

Summary

We have explored the conditions for instability through ion-beam oscillations in the Fermilab recycler ring. Multiturn and single-pass fast-ion modes have been discussed. The instability appears possible and may have been observed. Future observation will more clearly determine if the instability mode is actually occurring, and develop remedial action. The instability may be controlled by better vacuum, Landau damping, and an active transverse damper.

Acknowledgments

We gratefully acknowledge invaluable assistance from Dan Brousseliak, Sergei Nagaitsev, Cons Gattuso, Dave Johnson, Stan Pruss, and Steve Werkema.

Table 1 –Recycler Ring reference parameters.

Parameter	**Symbol**	**Value**	**Units**
Circumference	$L_{RR} = C_{RR}=2\pi R$	3320	m
Reference Momentum	$P_{\bar{p}}$	8.89	GeV/c
Transition slip factor	γ_T	20.0	
Betatron Tunes	ν_x, ν_y or Q_x, Q_y	25.4, 24.4	
Betatron Function values	β_{max},$\beta_{min,}$ β_{ave}	55, 15, 30	m
Reference emittance	$\varepsilon_{N,rms}$	1.6	mm-mrad
Reference beam sizes	σ_{max}, σ_{min}, σ_{ave}	3.06,1.6, 2.24	mm
Reference bunch length	L_B	2400	m
Beam pipe height, width	2a, 2b	4.5, 9	cm

Figures

Figure 1. Recycler betatron functions: β_x, β_y, η.

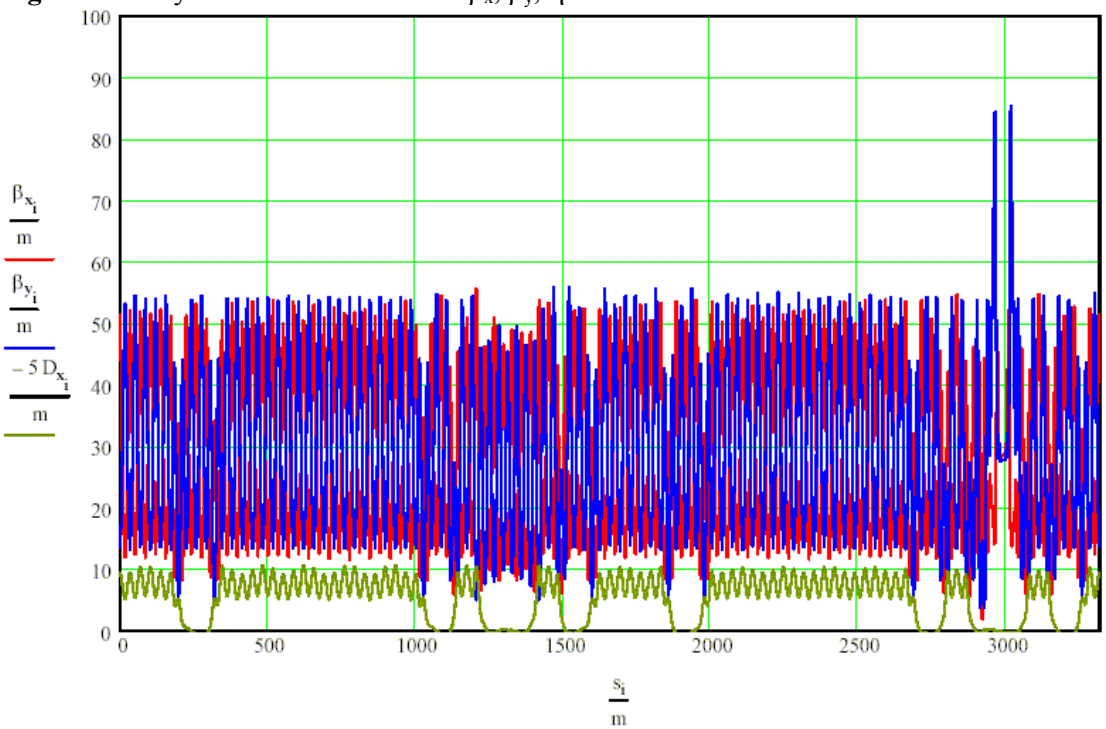

Figure 2: Space charge potential under assumption of round beam with constant density (red) or a Gaussian distribution (blue). Distributions are normalized to have the same charge and same rms radius. The horizontal axis is distance is in units of σ_r, with the beam pipe located at r = 10 σ_r. The vertical axis is the voltage, normalized to $\lambda/2\pi\varepsilon_0 = 1$.

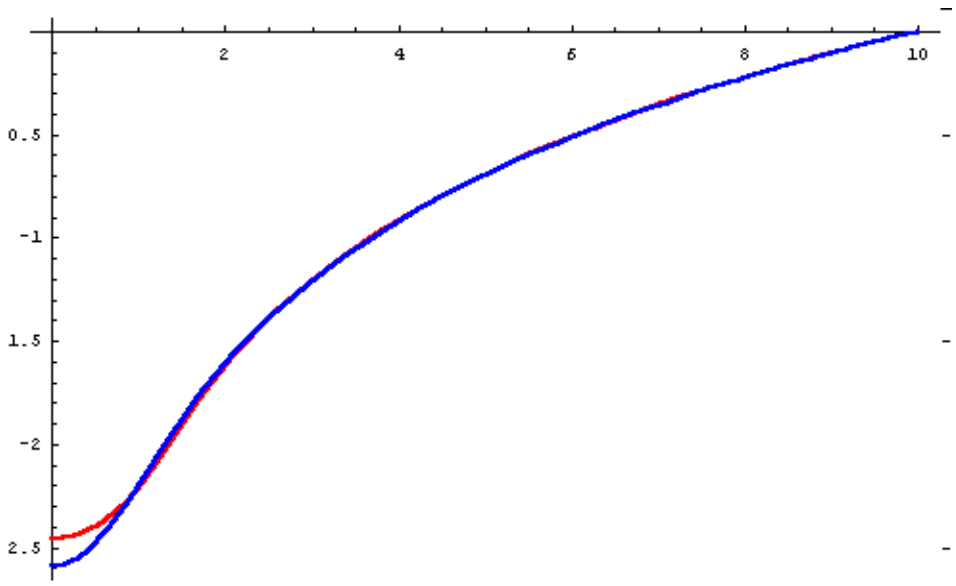

Figure 3: CO^+ ion oscillation frequencies (horizontal and vertical) in MHz around the ring (small oscillation frequencies at $N_{\bar{p}} = 20\times10^{10}$, $L_{bunch} = 2400$m, $\varepsilon_{N,rms} = 1.6$ πmm-mrad). In this calculation the beampipe aperture was assumed constant around the ring.

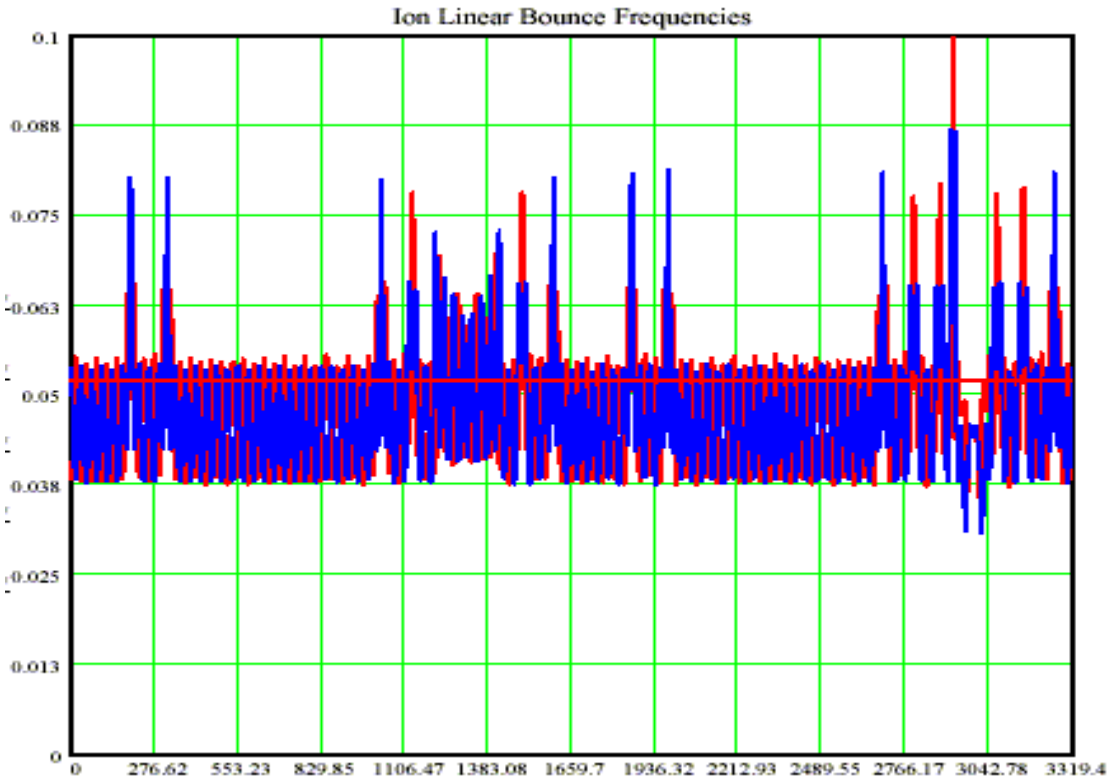

Figure 4. Trapping voltage around the RR, with $N_{\bar{p}} = 20\times10^{10}$, $L_{bunch} = 2400$m, $\varepsilon_{N,rms} = 1.6$ mm-mrad, and a 4.5×9cm beam pipe. Maximum trapping voltage is, typically, where beam is small vertically. The horizontal scale is 0 to 3320m (RR circumference), and vertical scale is 0.6 to 0.9 V.

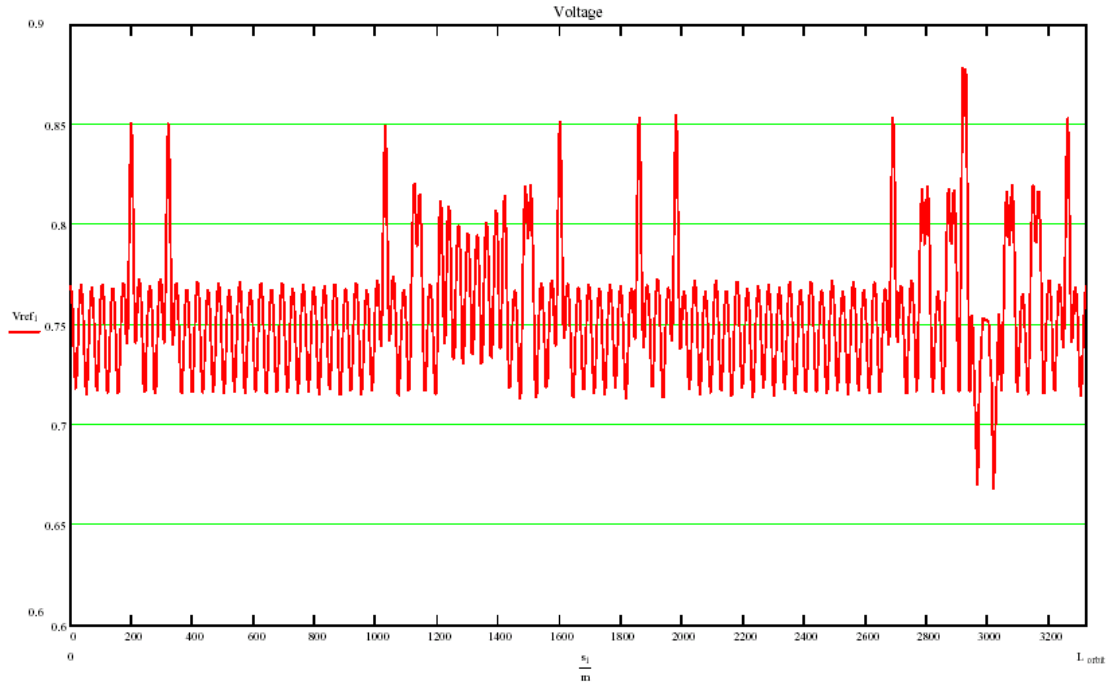

Figure 5: Overview of multiturn ion trapping scenario. The beam passes through the background gas, ionizing some atoms that are trapped within the beam field. A beam-free gap follows, in which ions no longer have a trapping potential, followed by another pass of beam which attracts the ions. If the total effect of bunching and beam-free drift is stably attractive, ions remain trapped over multiple turns and can accumulate to high density. If it is unstable, ions are lost in a few turns, and cannot accumulate to high density.

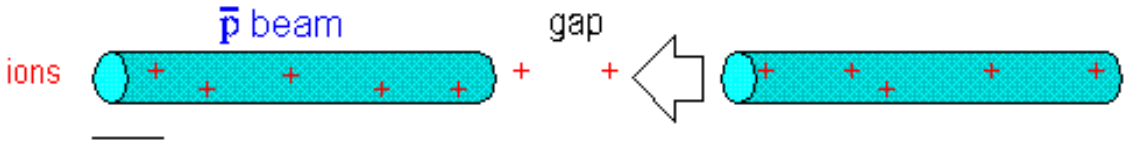

Figure 6. Half-trace ($|TrM|/2$) of x and y trapped-ion transport for N= 20×10^{10}, L_{beam} = 2000m, $\varepsilon_{x,rms} = \varepsilon_{y,rms}$ = 1.67 mm-mrad. Ions are trapped if the half trace is <1 for both x and y motion. This is true for a relatively small fraction of the ring at these parameters (~10%).

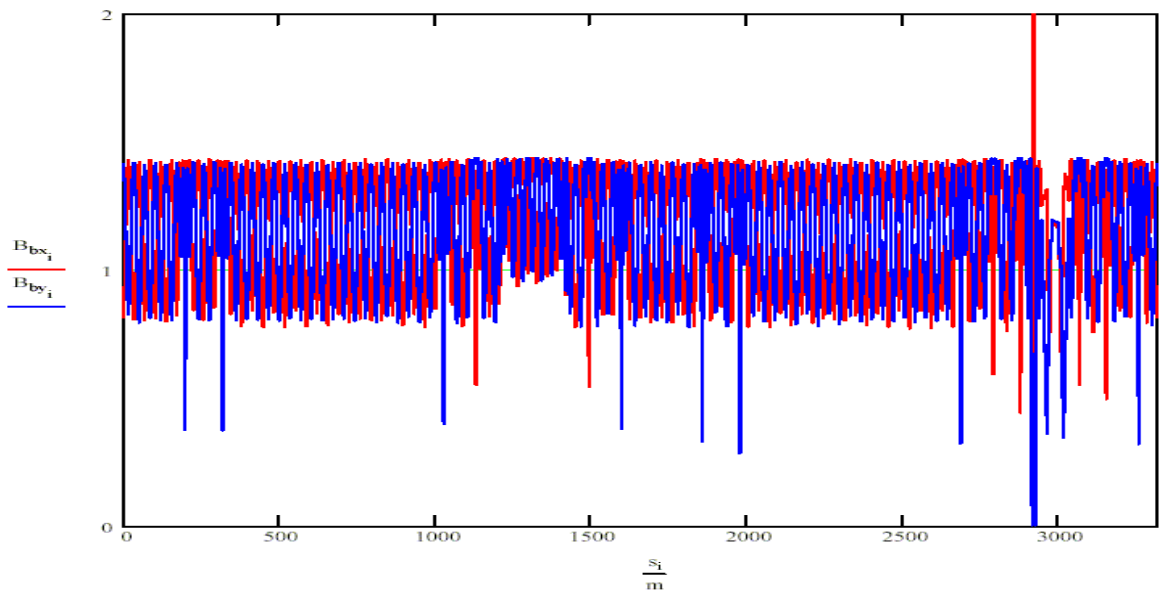

Figure 7: Situation for "fast-ion instability"; beam; ions build up within the beampipe as the beam passes from head to tail; instability develops toward the end of the bunch. Ions clear after beam passes by.

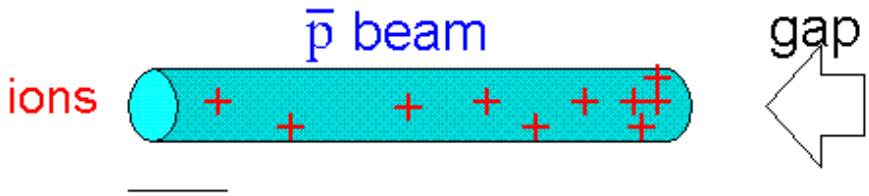

Figure 8: Growth of amplitude in fast beam ion instability as a function of the parameter η_{SC}. (from ref. [22]) Significant oscillation growth requires $\eta_{SC} > \sim 3$.

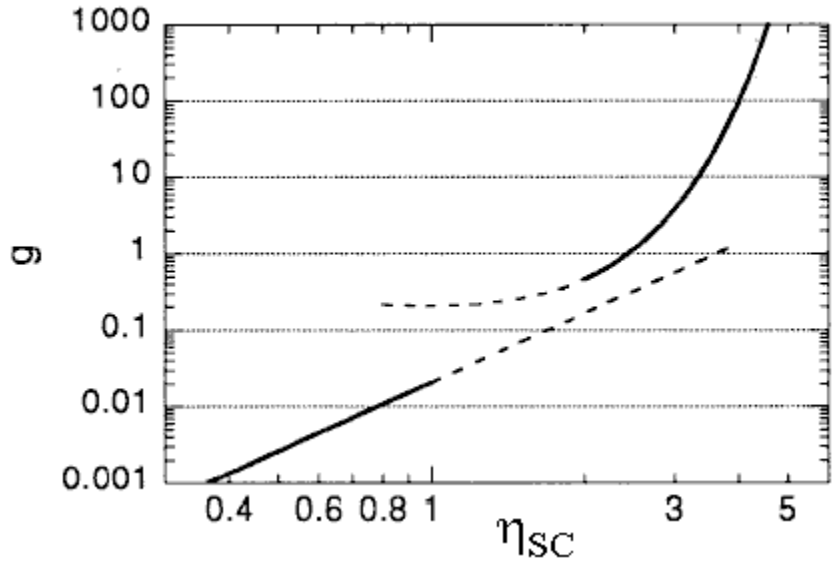

Figure 9: – Slow transverse emittance growth instability. Data taken with $N_{\bar{p}}$ =19.7 $10^{10}$and δE_{rms} = 1MeV, and cooling and clearing systems off. At t=0s, the rf is turned off, and the beam transverse emittances more than double in ~300s. Clearing voltages switched from 0 to 300 V at t ≅ 180s.

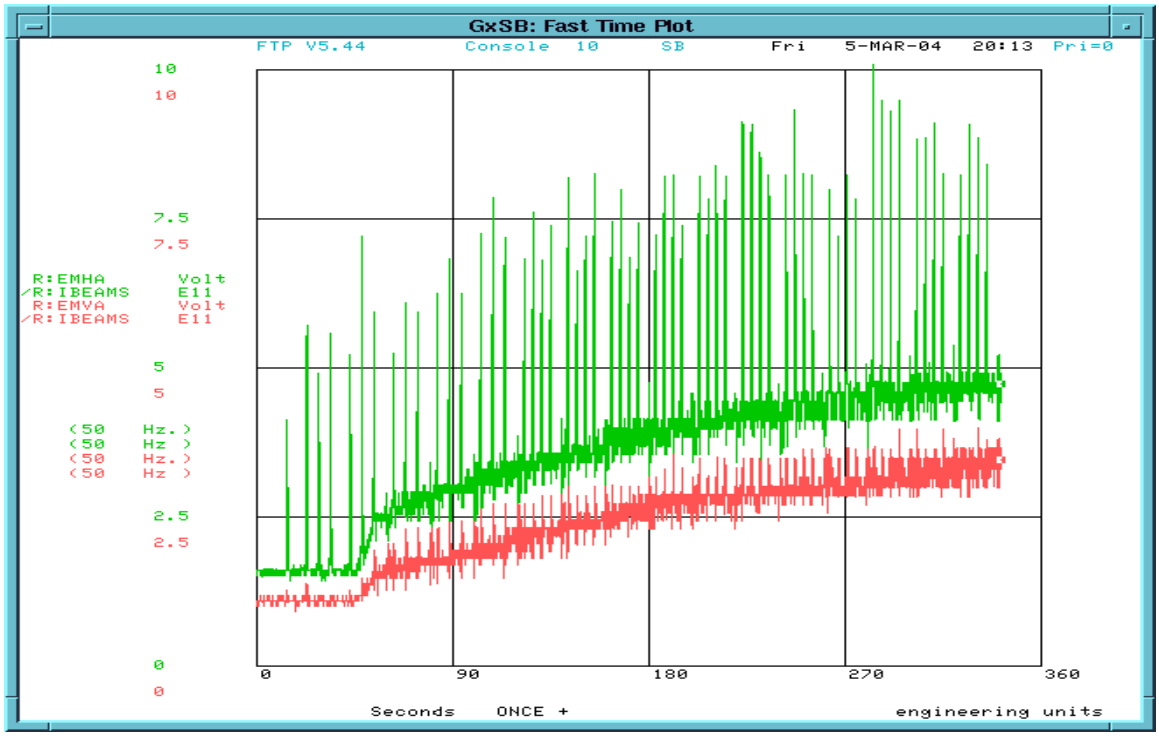

Figure 10: Fast-instability event, in which the beam rms emittance increases by a factor of ~2 in a fraction of a second, while some beam is lost (~5%)in a fraction of a second.

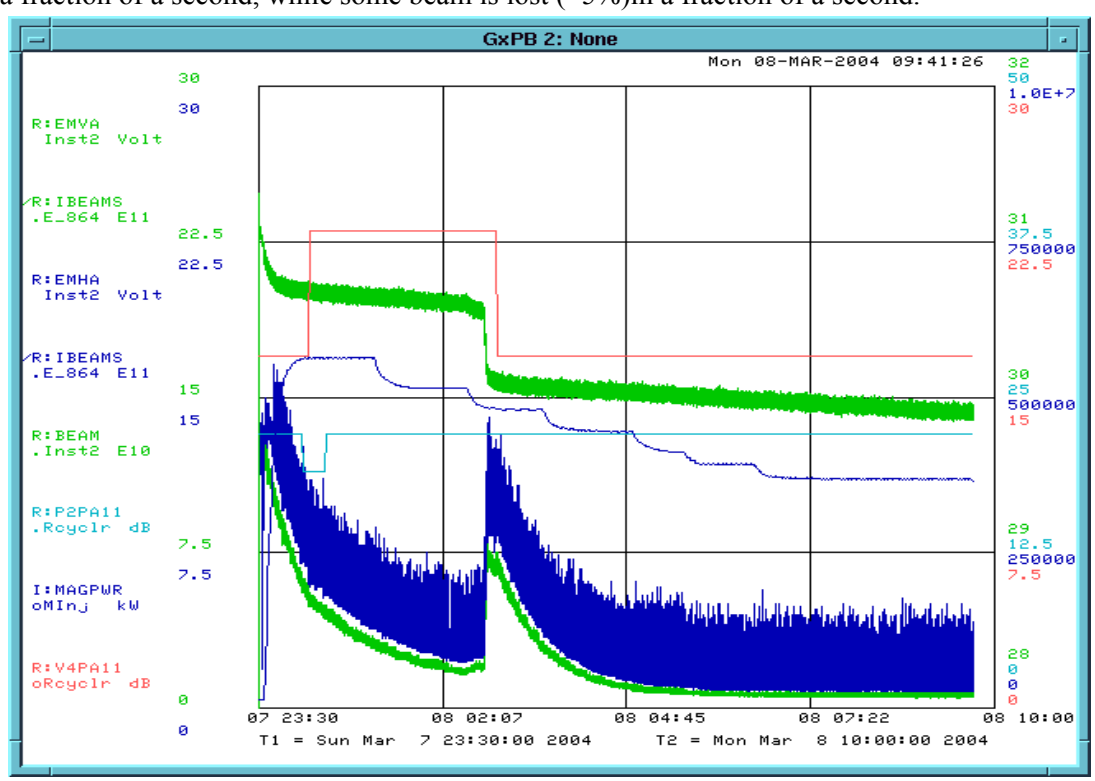

References

[1] A. Poncet, "Ion Trapping and Clearing", CAS Proc. CERN 95-06, p. 859 (1995).
[2] Y. Baconnier, A. Poncet, and P. F. Tavares, "Neutralisation of accelerator beams by Ionisation of the Residual Gas",CAS Proc. CERN 94-01, p. 525 (1994).
[3] A. Poncet, "Ions and Neutralization", in Frontiers of Particle Beams: Intensity Limitations, (M. Dienes, M. Month, S. Turner, eds.) Springer-Verlag LNP, p. 488 (1990).
[4] ibid., ref. 1.
[5] J. B. Rosenzweig and P. Zhou, "Coherent Beam-Ion Instabilities in the Fermilab Antiproton Accumulator," Proc. Fermilab III Instabilities Workshop, p. 9 (1990).
[6] Recycler Conceptual Design Study, G. Jackson, ed., Fermilab-TM-1936, July, 1995.
[7] F. Rieke and W. Prepejchal, Phys. Rev. A6, 1507 (1972).
[8] O. Grobner and K. Hubner, CERN/ISR-TH-VA/75/27 (1975).
[9] L. J. Laslett, BNL Report 7534,p.324 (1963).
[10] V. Balbekov, unpublished [2004].
[11] S. Werkema, K. D. Fullett, and P. Zhou, Proc. 1993 Part. Acc. Conf. , p. 3309 (1993).
[12] E. Keil and B. Zotter, CERN-ISR-TH/79-58 (1979).
[13] ibid., ref. 5.
[14] T. Raubenheimer and F. Zimmermann, Phys. Rev. E52, p. 5487 (1995).
[15] G. V. Stupakov, T. Raubenheimer and F. Zimmermann., Phys. Rev. E52, p. 5499 (1995).
[16] J. Byrd et al. , Phys Rev. Lett. 79, p.79 (1997)
[17] F. Zimmerman, Proc. EPAC2002, Paris, France, p. 25 (2002).
[18] A. Chao, unpublished (2002).
[19] G. V. Stupakov, Proc. Int. workshop on Collective Effects and Impedance for B-Factories, CEIBA95, KEK Proc. 96-6, p. 242 (1996).
[20] R. A. Bosch, Phys. Rev. Spec. Topics- AB 3, 034402 (2000).
[21] S. Heifets, Proc. Int. Workshop on Collective Effects and Impedance for B-Factories, CEIBA95, KEK Proc. 96-6, p. 270 (1996).
[22] A. W. Chao and G. V. Stupakov, SLAC-PUB-7607, Proc. Int. Workshop on Multi-bunch Instabilities, Tsukuba (1997).
[23] Fermilab log books, http://www-bd.fnal.gov/cgi-mach/machlog.pl?nb=recycle04&load=no, (2004).